Metabolic intervention by low carbohydrate diet suppresses the onset and progression of neuroendocrine tumors

Yu Chen[1], Tatsuki Yamamoto[1], Yura Takahashi[1], Tomoka Moro[1], Tomoko Tajima[1], Yukiko Sakaguchi[1], Naoaki Sakata[2], Akihiko Yokoyama[3], Susumu Hijioka[4], Akane Sada[1], Yuko Tabata[1] and Rieko Ohki[1,*]

[1] Laboratory of Fundamental Oncology, National Cancer Center Research Institute, Tsukiji 5-1-1, Chuo-ku, Tokyo 104-0045, Japan.

[2] Department of Regenerative Medicine and Transplantation, Faculty of Medicine, Fukuoka University, Nanakuma 7-45-1, Jonan-ku, Fukuoka, 814-0180, Japan.

[3] Tsuruoka Metabolomics Laboratory, National Cancer Center, Yamagata, 997-0052, Japan.

[4] Department of Hepatobiliary and Pancreatic Oncology, National Cancer Center Hospital, Tokyo 104-0045, Japan.

Running title: Repression of insulin signaling by dietary intervention suppresses neuroendocrine tumors

Key words: neuroendocrine tumor, non-functional pancreatic neuroendocrine tumor, MEN1, ketogenic diet, pituitary neuroendocrine tumor

*Correspondence:
Rieko Ohki; Tel: 81-3-3542-2511 ext. 3833, E-mail: rohki@ncc.go.jp

ABSTRACT

Insulin signaling often plays a role in the regulation of cancer including tumor initiation, progression, and response to treatment. In addition, the insulin-regulated PI3K-Akt-mTOR pathway plays an important role in the regulation of islet cell proliferation and this pathway is hyperactivated in human non-functional pancreatic neuroendocrine tumors (PanNETs). We therefore investigated the effect of a very low carbohydrate diet (ketogenic diet) on a mouse model that develops non-functional PanNETs to ask how reduced PI3K-Akt-mTOR signaling might affect the development and progression of non-functional PanNET. We found that this dietary intervention resulted in lower PI3K-Akt-mTOR signaling in islet cells and a significant reduction in PanNET formation and progression. We also found that this treatment had a significant effect on the suppression of pituitary NET development. Furthermore, we found that non-functional PanNET patients with lower blood glucose levels tend to have a better prognosis than patients with higher blood glucose levels. This preclinical study shows that a dietary intervention that results in lower serum insulin levels leads to lower insulin signal within the neuroendocrine cells and has a striking suppressive effect on the development and progression of both pancreatic and pituitary NETs.

Introduction

The pancreas serves two distinctly different functions as an exocrine organ and endocrine organ. As an endocrine organ, pancreatic islet cells release hormones and polypeptides, including insulin and glucagon, that regulate blood sugar levels and multiple other functions. When these pancreatic islet cells become cancerous, they are termed pancreatic neuroendocrine tumors (PanNETs). PanNETs are relatively rare tumors, comprising 1-2% of all pancreatic neoplasms and with an incidence of 0.43 per 100,000; however, this rate has more than doubled in the last 20-30 years [1]. The majority of PanNETs arise sporadically, but approximately 10% are associated with an underlying genetic syndrome [2]. PanNETs are divided into functional versus non-functional tumors with about 90% being classified as non-functional. Lesions should be surgically resected when possible, as this is the only potentially curative therapy. Liver metastasis is the most significant prognosis factor in the PanNET progression setting. Most patients, however, that have the metastatic disease are not candidates for resection. The majority of the drugs approved for the management of PanNET show little objective response, providing little progression-free survival or ability to shrink tumors, and thus PanNETs represent a serious unmet medical need in the clinic [3 4].

Some PanNETs arise due to a genetic disease called Multiple endocrine neoplasia type 1 (MEN1), an autosomal dominantly inherited tumor syndrome caused by germline mutations of the tumor suppressor gene *MEN1* [5]. PanNETs are the most prevalent NETs found in MEN1 patients, who will also develop NETs in other organs such as the pituitary; however, the development of a PanNET is a poor prognostic factor. Roughly 50% of patients are diagnosed with PanNETs under age 50, and since most patients have multiple non-functional PanNETs, surgery is not a therapeutic option [3]. The association between the loss of the *MEN1* gene function and the development of NETs has been confirmed by analyzing *Men1*-deficient mice [6]. The *Men1*$^{f/f}$-RipCre^{+} mouse in which *Men1* is ablated in pancreatic β-cells and pituitary cells is the most well-characterized MEN1 mouse model [7, 8]. These mice develop PanNETs and pituitary NETs and their use has contributed to a better understanding of these diseases in vivo. There are several independently derived β cell and pituitary cell-specific *Men1* knock-out mice that are similar but slightly different from one another [6, 9]. For example, β cell and pituitary cell-specific *Men1*-deficient mice that lack exons 3-8 develop PanNET by 15 months of age, while mice that lack exon 3 develop PanNET by 6 months [7, 8].

Insulin signaling plays a role in cancer including tumor initiation, progression and response to treatment [10]. Studies of some common cancers, such as breast and pancreatic cancers, have shown that hyperinsulinemia enhances tumor development in both humans and mice, while reduced insulin levels reduces tumor development [11 12 13 14]. Several preclinical studies in mice have shown that

79 dietary interventions leading to low insulin levels in the blood can enhance anticancer therapy and
80 improve the outcomes of several cancers [15 16]. It is of note that a diet that reduces the serum insulin
81 levels, i.e., a low-carbohydrate ketogenic diet, is safe and has no adverse effects in mice [17].
82
83 Pancreatic islets are exposed to high levels of insulin, which is released from β cells within the islets
84 [18]. In addition, it has been shown that the insulin-regulated PI3K-Akt-mTOR pathway plays an
85 important role in the regulation of islet cell proliferation and this pathway is hyperactivated in human
86 PanNETs [19 20 21]. We have previously shown that hyperactivation of the PI3K-Akt-mTOR pathway
87 caused by suppression of the tumor suppressor gene *PHLDA3*, which encodes a repressor of Akt,
88 contributes to the formation of hyperplastic islets in mouse models and to the progression of human
89 PanNETs [20 21 22 23 24]. These observations led us to investigate the effects of an insulin-lowering
90 diet on PanNET initiation and progression using a newly established non-functional PanNET mouse
91 model, which we fed with a very low carbohydrate diet (ketogenic diet). When fed a normal diet,
92 these mice develop non-functional PanNET by the age of 45 weeks, however when fed a very low
93 carbohydrate diet both initiation and progression of non-functional PanNET were significantly
94 suppressed. We also found that pituitary NET development in these mice is attenuated by a ketogenic
95 diet. We further showed that PanNET patients with higher blood glucose levels tend to have a poorer
96 prognosis than those with lower blood glucose levels. Collectively, these results suggest a novel
97 therapeutic and preventive approach of using a ketogenic diet to treat NET patients, including sporadic
98 and familial non-functional PanNET and pituitary NET patients. This treatment has shown no
99 adverse effects and provides a novel method to fulfill the unmet medical needs of non-functional
100 PanNET and pituitary NET patients.

Results

β cell-specific *Men1* knock-out mice that lack the exons 3-6 develop non-functional PanNETs

We made a β cell-specific *Men1* conditional knock-out mouse line by crossing *Men1* exons 3-6 floxed mice with RIP-Cre mice (*Men1*$^{f/f}$-RipCre^{+}) [25]. Similar to previous reports, nearly all of these mice developed PanNET by 10 months of age (Fig. 1A). As shown in Figs. 1B-1D, we found that the body weights, blood glucose levels and serum insulin levels in these mice are similar to those of wild-type mice at the same age. However, insulin expression is reduced in the islets of the *Men1*$^{f/f}$-RipCre^{+} mice at 10 months compared to the wild-type mice at the same age (Fig. 1E). It was previously reported that β cell-specific, *Men1*-deficient mice that lack exons 3-8 or exon 3 develop functional insulinomas with significantly elevated levels of serum insulin levels [7, 8]. However, we found that the β cell-specific *Men1*-deficient mice we established develop non-functional PanNETs that resemble those found in human MEN1 patients.

A ketogenic diet suppresses PanNET development

We found that male mice lacking *Men1* exons 3-6 in β cells develop PanNET by the age of 45 weeks. These mice have almost no abnormalities at 10 weeks (Figs. 2A-2C). In order to analyze the effect of a ketogenic diet on non-functional PanNET development, we started feeding the *Men1*$^{f/f}$-RipCre^{+} male mice with a ketogenic diet from the age of 7-13 weeks. The mice were sacrificed at age 45 weeks and the sizes of the islets were analyzed. As shown in Figs. 2A-2C and S1, the ketogenic diet significantly suppressed the development of islet hyperplasia and PanNET. There was no significant difference in the sizes of the islets of the ketogenic diet-fed mice and wild-type mice at the same age (Fig. 2C). In addition, the sizes of the islets of *Men1*$^{f/f}$-RipCre^{+} mice fed the ketogenic diet were not significantly different from those of 10-week-old mice, showing that the ketogenic diet suppressed the enlargement of the islets during the first 35 weeks (Fig. 2C).

We next analyzed the features of the islets of the ketogenic diet-fed *Men1*$^{f/f}$-RipCre^{+} mice. As shown in Fig. 2D, islets from *Men1*$^{f/f}$-RipCre^{+} mice fed either a normal or ketogenic diet were both positive for the neuroendocrine marker chromogranin A and had lost the expression of Menin as expected. As shown in Fig. 1E, *Men1*-deficient islets at 45 weeks of age had decreased insulin expression. However, this decrease in islet insulin expression was rescued in mice fed a ketogenic diet (Figs. 2E and 2F). Collectively these results show that the ketogenic diet dramatically suppresses the onset of non-functional PanNET.

A ketogenic diet suppresses pancreatic islet cell proliferation.

The results indicate that the lower blood glucose levels resulting from a ketogenic diet also resulted in lower insulin levels in the blood and decreased insulin signaling in islet cells. We first analyzed the

137 body weights and blood glucose levels in 45-week-old mice fed a normal versus ketogenic diet ad
138 libitum. As shown in Figs. 3A and 3B, blood glucose levels were significantly lower in the mice fed
139 a ketogenic diet, while there were no significant differences in body weights. We next performed a
140 food tolerance test using fasted mice and analyzed blood glucose and serum insulin levels 1.5 hrs post
141 food intake. In the case of wild-type mice, blood glucose levels continue to decrease during the first
142 48 hours of fasting, while liver glycogen is not completely depleted until 36 hours of fasting [26, 27].
143 Based on these findings, we implemented a fasting period from overnight to 41 hours in our study to
144 minimize the effects of endogenous glucose. While there was a significant increase in blood glucose
145 and high insulin secretion in the mice refed a normal diet, these increases in blood glucose and insulin
146 were not detected in mice fed a ketogenic diet (Figs. 3C, 3D and S2). It was also shown that the
147 insulin-regulated PI3K-Akt-mTOR pathway (P-S6 and P-mTOR) is attenuated in the islet cells of mice
148 fed a ketogenic diet (Figs. 3E-3H). Since insulin signaling is closely related to islet cell proliferation,
149 it is expected that decreased insulin levels in the blood should result in decreased islet cell proliferation.
150 As shown in Figs. 3I-3K, the number of Ki67-positive proliferating cells is lower and the expression
151 of p27, a representative cell cycle inhibitor, was higher in the islets of mice fed a ketogenic diet. The
152 *Cdkn1b* gene encoding p27 is a target gene of Menin, and its mRNA expression was not affected by
153 the ketogenic diet, suggesting that p27 expression is regulated at the post-transcriptional level (Fig.
154 S3). These data show that the ketogenic diet suppressed the proliferation of *Men1*-deficient islet cells.
155
156 **A ketogenic diet changes microenvironment of the islet.**
157 It has been reported that angiogenesis is an important step in PanNET tumorigenesis and angiogenic
158 switch is turned on upon progression from hyperplasia to neoplasia [28]. Insulin signaling enhances
159 angiogenesis in the islets and PI3K-Akt-mTOR pathway has been shown to regulate angiogenesis [29]
160 [30]. Since we found that PI3K-Akt-mTOR pathway activation is suppressed by a ketogenic diet, we
161 analyzed whether a ketogenic diet reverses the vascularized phenotype of the PanNETs formed in
162 *Men1*$^{f/f}$-RipCre^{+} mice. As shown in Fig. 4A and 4B, while large blood vessels were frequently found
163 in the islets of the mice fed a normal diet, such vessels were highly reduced in the islets of the mice
164 fed a ketogenic diet. We further found that expression of angiogenic genes (Mmp-2 and Mmp-9)
165 were down regulated in the islets of the mice fed a ketogenic diet (Figs. 4C and 4D). Since it is
166 expected that suppression of angiogenesis in the islets will further change the microenvironment of
167 the islets, we further analyzed the expression of genes involved in macrophage activation (Il-1β and
168 Nos2). Expression of both genes were down regulated by ketogenic diet showing that macrophage
169 activation was suppressed by the diet (Figs. 4E and 4F). On the other hand, expression of the
170 endocrine marker Synaptophysin was not significantly different among the samples, indicating
171 consistency in islet isolation (Fig. 4G). Collectively, data show that a ketogenic diet suppresses
172 angiogenesis and macrophage activation, two important microenvironment involved in PanNET

173 progression.
174
175 **A ketogenic diet suppresses PanNET progression.**
176 As the ketogenic diet was found to suppress the onset and development of PanNETs in *Men1*$^{f/f}$-RipCre^{+}
177 mice, we next analyzed whether this diet also suppresses the progression of PanNETs. At 30 weeks
178 of age, *Men1*-deficient islets were found to be significantly larger than wild-type islets (Fig. 5A): the
179 average size of the largest 10 islets of *Men1*$^{f/f}$-RipCre^{+} mice at 30 weeks of age was 0.17 mm^2, while
180 those from wild type mice averaged 0.028 mm^2. We therefore started feeding the 30-week-old
181 *Men1*$^{f/f}$-RipCre^{+} mice a ketogenic diet. When the islet sizes were subsequently analyzed at age 45
182 weeks, the islet sizes of the mice fed a ketogenic from 30 weeks were significantly smaller than those
183 of mice fed a normal diet (Figs. 5B-5D and S4). Furthermore, the islet sizes were not significantly
184 different from those of 30-week-old *Men1*$^{f/f}$-RipCre^{+} mice, showing that the ketogenic diet suppressed
185 the progression of PanNET for 15 weeks when the mice were fed this diet. We also analyzed the
186 effect of the diet on islet cell proliferation and angiogenesis. As shown in Figs. 5E-5H, the ketogenic
187 diet significantly suppressed islet cell proliferation and angiogenesis further, indicating that the diet
188 significantly suppressed PanNET progression.
189
190 **A ketogenic diet suppresses pituitary NET development.**
191 *Men1*$^{f/f}$-RipCre^{+} mice develop not only PanNETs but also pituitary NETs. Pituitary NET
192 development is more enhanced in female mice and most of the female mice develop pituitary NETs
193 by the age of 45 weeks. We therefore analyzed the effect of a ketogenic diet on pituitary NET
194 development in 45-week-old female *Men1*$^{f/f}$-RipCre^{+} mice. We started feeding the *Men1*$^{f/f}$-RipCre^{+}
195 female mice with a ketogenic diet from the age of 10-13 weeks. As shown in Figs. 6A-6C, a
196 ketogenic diet significantly suppressed pituitary NET development in these mice. It has been
197 reported that *Men1*-deficient mice frequently develop prolactin-positive pituitary NETs. This
198 previous report was confirmed, and most of the *Men1*-deficient mice fed a normal diet developed
199 prolactin-positive tumors (Figs. 6D and 6E). Within the pituitary NET of the mouse fed a normal
200 diet, accumulation of prolactin-positive cells was observed, while no cells were positive for TSH,
201 another pituitary hormone. On the other hand, the distribution of prolactin- and TSH-producing cells
202 were similar to those of wild type mice, and the clonal expansion of prolactin- and TSH-producing
203 cells was not evident in the pituitaries of mice fed a ketogenic diet from 10 weeks of age (Figs. 6D
204 and 6E).
205 As shown in Fig. S5, the median survival of female *Men1*$^{f/f}$-RipCre^{+} mice is 56 weeks, and these mice
206 die from pituitary NETs. We, therefore, fed the mice a ketogenic diet to the age of 55 weeks and
207 analyzed the size of the pituitaries. As shown in Figs. 6F and 6G, ketogenic diet significantly
208 suppressed the pituitary NET development until the age of 55 weeks. The sizes of the pituitaries of

209 55-week-old mice were similar to those of the 45-week-old mice. Collectively, these results show
210 that a ketogenic diet also suppressed pituitary NET development and contribute to the extension of the
211 life of these mice.
212
213 **The relationship between PanNET patient prognosis and blood glucose level**
214 We next analyzed the relationship between overall survival and blood glucose levels in 54 patients
215 who had been pathologically diagnosed as having non-functional PanNETs (Grade 1-3) and those who
216 had undergone chemotherapy. Patients who developed multiple primary tumors were excluded from
217 the analysis. The American Diabetes Association has determined that a fasting blood glucose level
218 from 100 to 125 mg/dl is an indication of a prediabetic state [31]. Therefore, high blood glucose levels
219 were defined in our study as blood glucose levels higher than 100 mg/dl. The median blood glucose
220 levels in the low and high blood glucose groups were 92 mg/dl (76–100 mg/dl) and 117 mg/dl (101–
221 245 mg/dl), respectively, and in the high blood glucose level group, 16 (48%) of 33 patients had blood
222 glucose level greater than 125 mg/dl. As shown in Fig. 7A, there was a tendency for patients with
223 lower blood glucose levels to have a better prognosis (p=0.080). On the other hand, when major
224 clinicopathological characteristics are classified into low and high blood glucose level groups, as listed
225 in Fig. 7B, the distributions of age, sex and tumor grade were not significantly different between the
226 two groups. For patients who had undergone chemotherapy, there was no significant bias between
227 the blood glucose high and low groups for the various chemotherapeutic regimens, also listed in Fig.
228 7C. Collectively, these data suggest that high blood glucose induces the progression of PanNETs.
229

Discussion

In this study, we have shown that the metabolic intervention of a very low carbohydrate diet (ketogenic diet) could significantly suppress both the initiation and progression of non-functional PanNET and pituitary NET in a mouse model. Recent advances in the understanding of the molecular factors involved in pancreatic and pituitary NETs have led to new antitumor treatments, including reagents acting on specific molecular targets. For example, inhibitors of receptor tyrosine kinases and mTOR are in clinical use for the treatment of PanNETs, however they may have limited efficacy and patients often stop responding to these inhibitors [32]. The most frequently used PanNET mouse model used for preclinical testing of therapies is a RipTag2 mouse model, which expresses the SV40 T antigen under the control of insulin promoter and develops functional PanNETs [33]. There are also several independent β cell-specific *Men1* knock-out mice that develop functional insulinomas [7, 8 9]. With these functional PanNET mouse models, it has been shown that several molecular targeted drugs such as an anti-VEGF monoclonal antibody (targeting the angiogenic pathways) or nintedanib (targeting VEGF, PDGF, and fibroblast growth factor) have anti-tumorigenic effects [34 35 36]. However, there have been no preclinical studies involving mouse models of non-functional PanNETs. We have established a non-functional PanNET mouse model and shown that by maintaining low insulin signaling by a ketogenic diet, it is possible to prevent and suppress the progression of non-functional PanNETs. We have shown that this dietary intervention is also effective for pituitary NETs. Recently, it has been reported that the ketogenic diet may elicit its anticancer effect by acting on the cancer epigenome [37]. Analysis of ketogenic-diet-induced changes in the cancer epigenome is an interesting issue to be analyzed in future studies. It has also been reported that a low-carbohydrate ketogenic diet is safe and has no adverse effects in mice and can improve the effectiveness of some anticancer therapies [15 16 17]. Therefore, it would be of great interest in future studies to test combinations of a ketogenic diet with other anticancer therapies used for PanNETs and pituitary NETs.

The results shown in this study can be translated not only to sporadic but also to familial non-functional PanNETs and pituitary NETs. In MEN1 patients that develop familial NETs, non-functional PanNETs are highly prevalent and are the major cause of premature MEN1-related death[32]. Surgery has been the only curative option for nonfunctioning PanNETs, however, since MEN1 patients often have multiple PanNETs that occur at a younger age and have a higher metastatic potential, surgery is not always possible. Although clinical guidelines recommend early detection by genetic testing of asymptomatic relatives of MEN1-mutated patients within the first decade of life, there is currently no effective method of prevention for these patients. However, this preclinical study shows that dietary intervention with a very low carbohydrate diet is effective in preventing nonfunctioning PanNET in mice, and this method may be applicable to MEN1 patients.

This dietary intervention is effective not only for the prevention of PanNETs but also for the suppression of PanNET progression, and has no adverse side effects. We also showed that higher blood glucose levels are related to poorer prognosis of PanNET patients that are receiving chemotherapy. It has also been reported that high pre-operative blood glucose predicts a poor prognosis in PanNET patients [38]. In addition, metformin, a drug that reduces blood glucose levels, enhances the effect of chemotherapy in PanNET patients [39]. These results suggests that by lowering blood glucose, PanNET progression can also be suppressed in humans. Future clinical studies to investigate the effectiveness of this method for both familial and sporadic human non-functional PanNETs and pituitary NETs should be of great interest. It is also possible that this treatment could be applied to other types of cancers including various familial cancers that are dependent on the insulin-regulated PI3K-Akt-mTOR pathway, and could represent the first effective prevention method that does not have adverse effects.

Materials and Methods

Mice used in this study

Mouse experiments were performed in a specific pathogen-free environment at the National Cancer Center animal facility according to institutional guidelines and all the animal experiments were approved by the Committee for Ethics in Animal Experimentation at the National Cancer Center (T17-002-C01 and T17-011-M03). Mice were kept in an animal facility controlled at a temperature of 22±0.5°C, 45～65 % humidity, pressure difference of +10 to 20 Pa, ventilation of 15 or more air volumes per hour, class 10,000 clean room, 150 to 300 lux illumination (40 to 85 cm above the breeding room floor) and a 12 h light and dark cycle (8 am to 8 pm; light). Pancreatic β-cell-specific *Men1* deficient mice were generated by crossing mice carrying the floxed allele (*Men* $^{f/f}$) with RIP-Cre transgenic mice expressing the Cre recombinase under the control of the rat insulin II promoter (B6.Cg-Tg(Ins2-cre)25Mgn/J), termed *Men1*$^{f/f}$-RipCre^{+} mice [25 40]. The mice were backcrossed against C57BL6 at least 8 times before use in experiments. *Men1*$^{f/f}$-RipCre^{+} mice develop both PanNETs and pituitary NETs. While PanNET development is enhanced in male mice, pituitary NET development is more enhanced in female mice. By 45 weeks of age, most of the male mice develop PanNETs and most of the female mice develop pituitary NETs. We therefore analyzed the effect of a ketogenic diet on PanNETs in male mice and pituitary NETs in female mice. Mice were fed a normal diet (CE-2, Crea Japan, Tokyo, Japan) or Ketogenic AIN-76A-Modified Diet, High Fat, Paste (Bio-serv, NJ).

Blood glucose and Plasma Insulin Measurement.

Blood measurements were performed at 1-2pm. Blood glucose levels were determined with blood samples from tail vein punctures in mice using a Glucose pilot instrument (Aventir Biotech, Carlsbad, CA), according to the manufacturer's protocol. Plasma insulin levels were determined with blood samples from the inferior vena cava in mice using the Morinaga Ultra Sensitive Mouse Insulin Elisa Kit (Morinaga Institute of Biological Science, Inc., Tokyo, Japan), according to the manufacturer's protocol.

Immunohistochemistry (IHC)

IHC was performed basically as described according to the manufacturer's instructions [20]. In brief, after deparaffinization, tissues sections underwent antigen retrieval by autoclaving slides in 10 mM citrate buffer (pH 6.0). Sections were pretreated with 3 % H_2O_2 for inactivation of endogenous peroxidase. The primary antibodies used in the study were; rabbit anti-Ki67 monoclonal antibody (SP6, Novus Biologicals) diluted 1:200, rabbit anti-Chromogranin A polyclonal antibody (Thermo Scientific) diluted 1:200, rabbit anti-P-S6 (#5364, CST) diluted 1:500, rabbit anti-P-mTOR (#2976,

316 CST) diluted 1:100, rabbit anti-p27 (C19, Santacruz) diluted 1:1000, rabbit anti-rat Prolactin (the
317 Institute for Molecular and Cellular Regulation, Gunma University) diluted 1:5000, rabbit anti-rat
318 TSH (the Institute for Molecular and Cellular Regulation, Gunma University) diluted 1:5000. As
319 secondary antibodies, biotinylated anti-rabbit IgG antibody (VECTOR Laboratories) were used. We
320 also used SignalStain Boost Detection Reagent (HRP, Rabbit #8114) for CST antibodies. We used
321 3,3'-diaminobenzidine tetrahydrochloride (DAB; Muto Pure Chemicals) as the substrate chromogen.
322 The sections were counter-stained with hematoxylin. For fluorescent immunohistochemical staining
323 of insulin, glucagon and Menin, nonspecific interactions were blocked for 1h using a goat serum
324 solution. The primary antibodies were: guinea pig anti-insulin polyclonal antibody (Abcam) diluted
325 1:400, mouse anti-glucagon monoclonal antibody (SIGMA-ALDRICH) diluted 1:750, rabbit anti-
326 Menin polyclonal antibody (Bethyl Laboratories, A300-105A) diluted 1:3000 with Signal Enhancer
327 HIKARI (NACALAI TESQUE). These were applied to the slides and incubated overnight at 4 °C.
328 As secondary antibodies, Alexa Fluor 546 goat anti-rabbit IgG antibody (Invitrogen) diluted 1:500 and
329 Alexa Fluor 546 or 594 goat anti-guinea pig IgG antibody (Invitrogen) diluted 1:1000 with PBST-
330 BSA were applied to the slides and incubated 3 hrs at RT. For mouse antibodies, the Vector MOM
331 immunodetection kit was used based on the protocol specified by the manufacturer (Vector
332 Laboratories).
333
334 **Isolation of Mouse Islets.**
335 Isolation of mouse islets was performed as described [20]. Briefly, mouse islets were isolated from 45-
336 week-old male animals by collagenase digestion of the pancreas, followed by purification using a
337 Ficoll gradient. Islets were handpicked and used for the subsequent analysis as shown in Figs. 4C-
338 4G and S3.
339
340 **Reverse Transcription and Real-Time PCR.**
341 Total cellular RNA was extracted using AllPrep DNA/RNA/Protein mini kit (Qiagen, UK). Reverse
342 transcription was carried out using kits from Invitrogen following the manufacturer's instructions
343 (SuperScript First-Strand Synthesis System for RT-PCR). Total RNA (0.2–5 μg) was used for reverse
344 transcription. Reverse-transcribed cDNAs were subjected to realtime PCR, which was performed
345 for genes of interest by using the SYBR Green Premix ExTaq (Tli RNaseH Plus) (Takara bio Inc,
346 Japan) and the CFX96 Real-time PCR (Biorad, UK), according to manufacturer's instructions.
347 TaqMan probe for mouse 18S rRNA, β-actin and Il-1β from Integrated DNA Technologies and
348 custom-designed primers were used to detect Cdkn1b (F; AGCAGTGTCCAGGGATGAGGAA,
349 R; TTCTTGGGCGTCTGCTCCACAG), Mmp2 (F; CAAGGATGGACTCCTGGCACAT,
350 R; TACTCGCCATCAGCGTTCCCAT), Mmp9 (F; GCTGACTACGATAAGGACGGCA,
351 R; TAGTGGTGCAGGCAGAGTAGGA), Nos2 (F; GAGACAGGGAAGTCTGAAGCAC,

R; CCAGCAGTAGTTGCTCCTCTTC), Synaptophysin (F; CCTGTCCGATGTGAAGATGG, R; AGGTTCAGGAAGCCAAACAC) gene expression. Relative gene expression levels were obtained by normalization to the expression levels of 18S ribosomal RNA (Cdkn1b and Synaptophysin) or β-actin (Mmp9, Mmp2, Nos2, Il-1β).

Quantitative measurement of islet and pituitary morphology.

Islet area, islet nuclei number and pituitary area were measured from hematoxylin and eosin-stained pancreas sections, and Ki67-positive cells were counted from immunohistochemically stained pancreas sections using TissueFAXS (TissueGnostics) and an HS All-in-one Fluorescence microscope BZ-9000 (Keyence).

Quantification analysis of the HE and IHC images

Image analyses of Insulin, P-S6, P-mTOR, Ki67, and p27 were performed using ImageJ software (imageJ.net). Additionally, color thresholding image adjustment was performed with the Colour Deconvolution plugin (imagej.net/Colour_Deconvolution). We used an optimized immunohistochemistry image processing protocol for DAB staining to semi-quantitatively analyze protein expression, as previously described [41]. Image analyses of vessels were also done using ImageJ software. Images analyses of Figs. S1 and S4 were analyzed with an HS All-in-one Fluorescence microscope BZ-9000 (KEYENCE).

Patients analyzed in the study.

A retrospective cohort study was conducted consisting of 56 patients who had been pathologically diagnosed with PanNETs and those that had undergone chemotherapy without surgery between July 2014 to August 2021 at National Cancer Center Hospital. Only data from patients who did not receive prior chemotherapy were included, and blood collection was performed before therapy. We did not include patients who had undergone chemotherapy, as these treatments can potentially affect pancreatic function. Some patients had undergone previous surgery and only those who were one year or more post-surgery were included in the analysis. There was no significant difference in the blood glucose levels between the patients with or without surgery (Fig. S6). Chemotherapies included: octreotide, lanreotide, everolimus, sunitinib, streptozotocin, lanreotide+everolimus, lanreotide+sunitinib and others (CDDP+CPT-11, GEM+nabPTX or PRRT). Inclusion criteria were as follows: (i) patients diagnosed with PanNET; (ii) patients with follow-up data; (iii) patients with blood glucose data before the treatments. Cases excluded were (i) patients diagnosed with functional PanNETs or (ii) patients that had developed multiple primary tumors. This study was approved by the Institutional Review Board of the National Cancer Center, Tokyo (approval number; 2013-023). Informed consent was obtained for all cases. Clinical and pathological data were obtained through a

388 detailed retrospective review of the medical records of all patients with PanNET. According to the
389 Standards of Medical Care in Diabetes 2022 issued by the American Diabetes Association [31], a fasting
390 blood glucose (FBG) level from 100 to 125 mg/dl is an indication of a prediabetic state. Therefore,
391 high blood glucose levels are defined as blood glucose levels higher than 100 mg/dl. Overall survival
392 (OS) was defined as the length of time (in days) from the beginning of treatment to death from any
393 cause.
394
395 **Statistical analysis.**
396 Data were calculated and shown as mean ±SEM. Comparisons between the samples were performed
397 by Student *t* test or by one-way ANOVA multiple comparisons (Tukey's multiple comparisons test)
398 using Prism software (version 6). For the t test, Student's t test was used when the variances of the
399 groups were not significantly different as evaluated by f test. Survival data were analyzed using
400 Prism software (version 6), and Kaplan–Meyer plots were drawn. Statistical significance was
401 defined as $p<0.05$. For animal studies, no statistical methods were used for sample size estimate, no
402 samples were excluded, no randomization was used, and no blinding was done.
403

CONFLICT OF INTEREST

The authors state no conflict of interest.

ACKNOWLEDGMENTS

We thank Dr. Marc Lamphier for critical reading of the manuscript. Y.C. is a JSPS International Research fellow. This work was carried out by the joint research program of the Institute for Molecular and Cellular Regulation, Gunma University. This study was partly supported by a Grant-in-Aid for Scientific Research (B, #20H03523 to R.O.), Grant-in-Aid for Scientific Research (C, #22K07181 to Yuko T.) and Grant-in-Aid for Young Scientist (B) (#19K16732 to Y.C.) from MEXT of Japan; P-Direct and P-Create from AMED of Japan (R.O.); Grant-in-Aid for JSPS fellow (# 20F20414 to R.O. and Y.C.); research grants of the Okinaka Memorial Institute for Medical Research (R.O.), the Life Science Foundation of Japan (R.O.), Pancreas Research Foundation of Japan (Y.C.) and Ichiro Kanehara Foundation for the promotion of Medical Sciences and Medical Care (Y.C.).

AUTHOR CONTRIBUTIONS

Conceptualization: RO; Formal Analysis: YC, TY, YuraT, TM, TT, YS, NS, SH, AS, YukoT, RO; Investigation and Methodology: YC, TY, YuraT, TM, TT, YS, NS, AY, SH, AS, YukoT, RO; Funding acquisition: YC, YukoT, RO; Supervision: RO; Writing – original draft; RO, review & editing: YC, TY, YuraT, TM, TT, YS, NS, AY, SH, AS, YukoT, RO.

References

1. McKenna LR, Edil BH. Update on pancreatic neuroendocrine tumors. *Gland Surg* 2014, **3**(4)**:** 258-275.

2. de Wilde RF, Edil BH, Hruban RH, Maitra A. Well-differentiated pancreatic neuroendocrine tumors: from genetics to therapy. *Nat Rev Gastroenterol Hepatol* 2012, **9**(4)**:** 199-208.

3. Mpilla GB, Philip PA, El-Rayes B, Azmi AS. Pancreatic neuroendocrine tumors: Therapeutic challenges and research limitations. *World J Gastroenterol* 2020, **26**(28)**:** 4036-4054.

4. Jensen RT, Bodei L, Capdevila J, Couvelard A, Falconi M, Glasberg S*, et al.* Unmet Needs in Functional and Nonfunctional Pancreatic Neuroendocrine Neoplasms. *Neuroendocrinology* 2019, **108**(1)**:** 26-36.

5. van Treijen MJC, van Beek DJ, van Leeuwaarde RS, Vriens MR, Valk GD. Diagnosing Nonfunctional Pancreatic NETs in MEN1: The Evidence Base. *J Endocr Soc* 2018, **2**(9)**:** 1067-1088.

6. Wiedemann T, Pellegata NS. Animal models of multiple endocrine neoplasia. *Mol Cell Endocrinol* 2016, **421:** 49-59.

7. Crabtree JS, Scacheri PC, Ward JM, McNally SR, Swain GP, Montagna C*, et al.* Of mice and MEN1: Insulinomas in a conditional mouse knockout. *Mol Cell Biol* 2003, **23**(17)**:** 6075-6085.

8. Bertolino P, Tong WM, Herrera PL, Casse H, Zhang CX, Wang ZQ. Pancreatic beta-cell-specific ablation of the multiple endocrine neoplasia type 1 (MEN1) gene causes full penetrance of insulinoma development in mice. *Cancer Res* 2003, **63**(16)**:** 4836-4841.

9. Gaspar TB, Lopes JM, Soares P, Vinagre J. An update on genetically engineered mouse models of pancreatic neuroendocrine neoplasms. *Endocr Relat Cancer* 2022, **29**(12)**:** R191-R208.

10. Hopkins BD, Goncalves MD, Cantley LC. Insulin-PI3K signalling: an evolutionarily insulated metabolic driver of cancer. *Nat Rev Endocrinol* 2020, **16**(5)**:** 276-283.

11. Novosyadlyy R, Lann DE, Vijayakumar A, Rowzee A, Lazzarino DA, Fierz Y*, et al.* Insulin-

460 mediated acceleration of breast cancer development and progression in a nonobese model of type
461 2 diabetes. *Cancer Res* 2010, **70**(2)**:** 741-751.
462
463 12. Gallagher EJ, LeRoith D. Hyperinsulinaemia in cancer. *Nat Rev Cancer* 2020, **20**(11)**:** 629-644.
464
465 13. Nencioni A, Caffa I, Cortellino S, Longo VD. Fasting and cancer: molecular mechanisms and
466 clinical application. *Nat Rev Cancer* 2018, **18**(11)**:** 707-719.
467
468 14. Zhang AMY, Magrill J, de Winter TJJ, Hu X, Skovso S, Schaeffer DF*, et al.* Endogenous
469 Hyperinsulinemia Contributes to Pancreatic Cancer Development. *Cell Metab* 2019, **30**(3)**:** 403-
470 404.
471
472 15. Hopkins BD, Pauli C, Du X, Wang DG, Li X, Wu D*, et al.* Suppression of insulin feedback
473 enhances the efficacy of PI3K inhibitors. *Nature* 2018, **560**(7719)**:** 499-503.
474
475 16. Taylor SR, Falcone JN, Cantley LC, Goncalves MD. Developing dietary interventions as therapy
476 for cancer. *Nat Rev Cancer* 2022.
477
478 17. Douris N, Melman T, Pecherer JM, Pissios P, Flier JS, Cantley LC*, et al.* Adaptive changes in
479 amino acid metabolism permit normal longevity in mice consuming a low-carbohydrate ketogenic
480 diet. *Biochim Biophys Acta* 2015, **1852**(10 Pt A)**:** 2056-2065.
481
482 18. Johnson JD, Alejandro EU. Control of pancreatic beta-cell fate by insulin signaling: The sweet
483 spot hypothesis. *Cell Cycle* 2008, **7**(10)**:** 1343-1347.
484
485 19. Elghazi L, Balcazar N, Bernal-Mizrachi E. Emerging role of protein kinase B/Akt signaling in
486 pancreatic beta-cell mass and function. *Int J Biochem Cell Biol* 2006, **38**(2)**:** 157-163.
487
488 20. Ohki R, Saito K, Chen Y, Kawase T, Hiraoka N, Saigawa R*, et al.* PHLDA3 is a novel tumor
489 suppressor of pancreatic neuroendocrine tumors. *Proc Natl Acad Sci U S A* 2014, **111**(23)**:** E2404-
490 2413.
491
492 21. Chen Y, Ohki R. p53-PHLDA3-Akt Network: The Key Regulators of Neuroendocrine
493 Tumorigenesis. *Int J Mol Sci* 2020, **21**(11).
494
495 22. Kawase T, Ohki R, Shibata T, Tsutsumi S, Kamimura N, Inazawa J*, et al.* PH domain-only protein

496 PHLDA3 is a p53-regulated repressor of Akt. *Cell* 2009, **136**(3)**:** 535-550.
497
498 23. Sakata N, Yamaguchi Y, Chen Y, Shimoda M, Yoshimatsu G, Unno M*, et al.* Pleckstrin homology-
499 like domain family A, member 3 (PHLDA3) deficiency improves islets engraftment through the
500 suppression of hypoxic damage. *PLoS One* 2017, **12**(11)**:** e0187927.
501
502 24. Takikawa M, Ohki R. A vicious partnership between AKT and PHLDA3 to facilitate
503 neuroendocrine tumors. *Cancer Sci* 2017, **108**(6)**:** 1101-1108.
504
505 25. Hughes CM, Rozenblatt-Rosen O, Milne TA, Copeland TD, Levine SS, Lee JC*, et al.* Menin
506 associates with a trithorax family histone methyltransferase complex and with the hoxc8 locus.
507 *Mol Cell* 2004, **13**(4)**:** 587-597.
508
509 26. Hashimoto T, Cook WS, Qi C, Yeldandi AV, Reddy JK, Rao MS. Defect in peroxisome
510 proliferator-activated receptor alpha-inducible fatty acid oxidation determines the severity of
511 hepatic steatosis in response to fasting. *J Biol Chem* 2000, **275**(37)**:** 28918-28928.
512
513 27. Lopez-Soldado I, Bertini A, Adrover A, Duran J, Guinovart JJ. Maintenance of liver glycogen
514 during long-term fasting preserves energy state in mice. *FEBS Lett* 2020, **594**(11)**:** 1698-1710.
515
516 28. Folkman J, Watson K, Ingber D, Hanahan D. Induction of angiogenesis during the transition from
517 hyperplasia to neoplasia. *Nature* 1989, **339**(6219)**:** 58-61.
518
519 29. Ulanet DB, Ludwig DL, Kahn CR, Hanahan D. Insulin receptor functionally enhances multistage
520 tumor progression and conveys intrinsic resistance to IGF-1R targeted therapy. *Proc Natl Acad Sci*
521 *U S A* 2010, **107**(24)**:** 10791-10798.
522
523 30. Allen E, Mieville P, Warren CM, Saghafinia S, Li L, Peng MW*, et al.* Metabolic Symbiosis
524 Enables Adaptive Resistance to Anti-angiogenic Therapy that Is Dependent on mTOR Signaling.
525 *Cell Rep* 2016, **15**(6)**:** 1144-1160.
526
527 31. American Diabetes Association Professional Practice C. 2. Classification and Diagnosis of
528 Diabetes: Standards of Medical Care in Diabetes-2022. *Diabetes Care* 2022, **45**(Suppl 1)**:** S17-
529 S38.
530
531 32. Brandi ML, Agarwal SK, Perrier ND, Lines KE, Valk GD, Thakker RV. Multiple Endocrine

532 Neoplasia Type 1: Latest Insights. *Endocr Rev* 2021, **42**(2)**:** 133-170.
533
534 33. Hanahan D. Heritable formation of pancreatic beta-cell tumours in transgenic mice expressing
535 recombinant insulin/simian virus 40 oncogenes. *Nature* 1985, **315**(6015)**:** 115-122.
536
537 34. Casanovas O, Hicklin DJ, Bergers G, Hanahan D. Drug resistance by evasion of antiangiogenic
538 targeting of VEGF signaling in late-stage pancreatic islet tumors. *Cancer Cell* 2005, **8**(4)**:** 299-
539 309.
540
541 35. Sennino B, Ishiguro-Oonuma T, Wei Y, Naylor RM, Williamson CW, Bhagwandin V*, et al.*
542 Suppression of tumor invasion and metastasis by concurrent inhibition of c-Met and VEGF
543 signaling in pancreatic neuroendocrine tumors. *Cancer Discov* 2012, **2**(3)**:** 270-287.
544
545 36. Bill R, Fagiani E, Zumsteg A, Antoniadis H, Johansson D, Haefliger S*, et al.* Nintedanib Is a
546 Highly Effective Therapeutic for Neuroendocrine Carcinoma of the Pancreas (PNET) in the
547 Rip1Tag2 Transgenic Mouse Model. *Clin Cancer Res* 2015, **21**(21)**:** 4856-4867.
548
549 37. Muscogiuri G, Barrea L, Campolo F, Sbardella E, Sciammarella C, Tarsitano MG*, et al.* Ketogenic
550 diet: a tool for the management of neuroendocrine neoplasms? *Crit Rev Food Sci Nutr* 2022, **62**(4)**:**
551 1035-1045.
552
553 38. Gong Y, Fan Z, Zhang P, Qian Y, Huang Q, Deng S*, et al.* High pre-operative fasting blood glucose
554 levels predict a poor prognosis in patients with pancreatic neuroendocrine tumour. *Endocrine* 2021,
555 **71**(2)**:** 494-501.
556
557 39. Vitali E, Boemi I, Tarantola G, Piccini S, Zerbi A, Veronesi G*, et al.* Metformin and Everolimus:
558 A Promising Combination for Neuroendocrine Tumors Treatment. *Cancers (Basel)* 2020, **12**(8).
559
560 40. Postic C, Shiota M, Niswender KD, Jetton TL, Chen Y, Moates JM*, et al.* Dual roles for
561 glucokinase in glucose homeostasis as determined by liver and pancreatic beta cell-specific gene
562 knock-outs using Cre recombinase. *J Biol Chem* 1999, **274**(1)**:** 305-315.
563
564 41. Capodanno Y, Chen Y, Schrader J, Tomosugi M, Sumi S, Yokoyama A*, et al.* Cross-talk among
565 MEN1, p53 and Notch regulates the proliferation of pancreatic neuroendocrine tumor cells by
566 modulating INSM1 expression and subcellular localization. *Neoplasia* 2021, **23**(9)**:** 979-992.
567

568 **Figure legends**

569

570 **Fig. 1 β cell-specific *Men1* knock-out mice develop non-functional PanNETs**

571 **A.** Pancreatic sections of 45-week-old wild-type mice and *Men1*$^{f/f}$-RipCre^{+} mice fed a normal diet
572 were stained with HE.

573 **B, C.** Body weights (B) and blood glucose levels (C) of 45-week-old wild-type (N=19) or *Men1*$^{f/f}$-
574 RipCre^{+} (N=21) mice fed a normal diet. Mice were fed ad libitum. Data are represented as the
575 mean fold expression ± standard error of the mean (SEM).

576 **D.** Serum insulin levels of 45-week-old wild-type (N=19) or *Men1*$^{f/f}$-RipCre^{+} mice fed a normal diet
577 (N=18). Mice were fed ad libitum. Data are represented as the mean fold expression ± SEM.

578 **E.** Pancreatic sections of 45-week-old wild-type or *Men1*$^{f/f}$-RipCre^{+} mice fed a normal diet were
579 stained with anti-insulin, anti-glucagon and anti-Chromogranin A.

580

581 **Fig. 2 Ketogenic diet suppresses non-functional PanNET development.**

582 **A.** Pancreatic sections of 45-week-old wild-type mice fed a normal diet, *Men1*$^{f/f}$-RipCre^{+} mice fed a
583 normal diet or *Men1*$^{f/f}$-RipCre^{+} mice fed a ketogenic diet from 8 weeks of age were stained with HE.
584 HE staining of pancreatic sections of 10-week-old *Men1*$^{f/f}$-RipCre^{+} mice fed a normal diet is also
585 shown.

586 **B.** Islet areas of 45-week-old wild-type mice fed a normal diet (N=6), *Men1*$^{f/f}$-RipCre^{+} mice fed a
587 normal diet (N=14) or *Men1*$^{f/f}$-RipCre^{+} mice fed a ketogenic diet from 7-13 weeks of age (N=13), and
588 10-week-old *Men1*$^{f/f}$-RipCre^{+} mice fed a normal diet (N=4) were analyzed. The areas of the top 10
589 largest islets were calculated and the means of the 10 islet areas were obtained for each mouse. Data
590 are represented as the mean fold expression ± standard deviation (SD).

591 **C.** Statistical analysis of the average islet sizes of each group of mice was performed. P values were
592 obtained using the one-way ANOVA test. The age of the mice sacrificed are shown in parenthesis.

593 **D.** Pancreatic sections of 45-week-old wild-type mice fed a normal diet, *Men1*$^{f/f}$-RipCre^{+} mice fed a
594 normal diet or ketogenic diet from 8 weeks of age were stained with HE, anti-Chromogranin A and
595 anti-Menin.

596 **E, F.** Pancreatic sections of 45-week-old wild-type mice fed a normal diet, *Men1*$^{f/f}$-RipCre^{+} mice fed
597 a normal diet or ketogenic diet from 8 weeks of age were stained with anti-insulin and anti-
598 Chromogranin A. Relative intensities of insulin staining from 3 mice of each group (total 9-12 islets)
599 were calculated and shown in Graph F. Data are represented as the mean fold expression SD.

600

601 **Fig. 3 Ketogenic diet suppresses pancreatic islet cell proliferation.**

602 **A, B.** Body weights (A) and blood glucose levels (B) of 45-week-old *Men1*$^{f/f}$-RipCre^{+} mice fed a
603 normal diet (N=18) or ketogenic diet (N=32). Mice were fed ad libitum. Data are represented as

604 the mean fold expression ± SEM.

605 **C, D.** Blood glucose levels (C) and serum insulin levels (D) of 20-week-old *Men1*$^{f/f}$-RipCre^{+} mice fed
606 a normal diet (N=4) or ketogenic diet from 10 weeks of age (N=3). Fasted mice (mice fasted for
607 overnight to 41 hrs) and mice refed the usual meal for 1.5 hrs were analyzed. Data are represented
608 as the mean fold expression ± SEM.

609 **E-G.** Mice were treated as in C and pancreatic sections of mice refed a normal diet or ketogenic diet
610 were stained with HE, anti-P-S6 (E) and anti-P-mTOR (F). High magnification images are shown in
611 the bottom panels. Relative intensities of P-S6 staining from 5 (normal diet) and 4 (ketogenic diet)
612 islets were calculated and shown in graph G. Relative intensities of P-mTOR staining from 4 (normal
613 diet) and 4 (ketogenic diet) islets were calculated and shown in graph H. Data are represented as the
614 mean fold expression ± SEM.

615 **I-K.** Pancreatic sections of 30-week-old *Men1*$^{f/f}$-RipCre^{+} mice fed a normal diet or ketogenic diet from
616 10 weeks of age were stained with HE, anti-Ki67 and anti-p27 (I). Total and Ki67 positive nuclei
617 numbers from 4 islets were counted and shown in Graph J. Relative intensities of p27 staining from
618 3 islets were calculated and shown in Graph K. Data are represented as the mean fold expression ±
619 SEM.

620

621 **Fig. 4 Ketogenic diet suppresses angiogenesis and macrophage activation.**

622 **A, B.** HE stained pancreatic sections of 45-week-old *Men1*$^{f/f}$-RipCre^{+} mice fed a normal diet (N=3) or
623 *Men1*$^{f/f}$-RipCre^{+} mice fed a ketogenic diet from 11 weeks of age (N=3) were analyzed. Typical
624 vascularized islet from the mice fed a normal diet and a non-vascularized islet from the mice fed a
625 ketogenic diet are shown (A). The number of vessels with an area of 0.0006 mm^2 or greater was
626 calculated from 4 fields derived from 4 islets from each mouse. The numbers of vessels are counted
627 and shown as a graph in B. Data are represented as the mean fold expression ±SD.

628 **C-G.** Islets were isolated from 45-week-old *Men1*$^{f/f}$-RipCre^{+} mice fed a normal diet or *Men1*$^{f/f}$-RipCre^{+}
629 mice fed a ketogenic diet from 10 weeks of age. 3 sets of islets were isolated from the mice fed a
630 normal diet (N=2, 2, 3) or mice fed a ketogenic diet from 10 weeks of age (N=2, 3, 7). mRNAs were
631 purified from islets and the expression of genes involved in angiogenesis (*Mmp2* and *Mmp9*) (C, D)
632 and macrophage activation (*Nos2* and *Il1β*) (E, F) were analyzed. An endocrine marker,
633 Synaptophysin, was also analyzed to evaluate the consistency of islet isolation (G). Data are
634 represented as the mean fold expression ± SD.

635

636 **Fig. 5 Ketogenic diet suppresses PanNET progression.**

637 **A.** Islet areas of 30-week-old wild-type mice and *Men1*$^{f/f}$-RipCre^{+} mice fed a normal diet were
638 analyzed. The areas of the top 10 largest islets were calculated and the means of the 10 islet areas
639 were obtained for each mouse. Data are represented as the mean fold expression ± SD.

640 **B.** Pancreatic sections of 45-week-old *Men1*$^{f/f}$-RipCre^{+} mice fed a normal diet or ketogenic diet from
641 30 weeks of age were stained with HE. HE staining of pancreatic sections of 30-week-old *Men1*$^{f/f}$-
642 RipCre^{+} mice fed a normal diet is also shown.
643 **C.** Islet areas of 45-week-old *Men1*$^{f/f}$-RipCre^{+} mice fed a normal diet or ketogenic diet from 30 weeks
644 of age, and 10- or 30-week-old *Men1*$^{f/f}$-RipCre^{+} mice fed a normal diet were analyzed as in A.
645 *Men1*$^{f/f}$-RipCre^{+} mice fed a normal diet is same as the mice described in Fig. 5A. Data are
646 represented as the mean fold expression ± SD.
647 **D.** Statistical analysis of the average islet sizes of each group of mice was performed. P values were
648 obtained using the one-way ANOVA test. The age of the mice sacrificed are shown in parenthesis.
649 **E, F.** Pancreatic sections of 45-week-old *Men1*$^{f/f}$-RipCre^{+} mice fed a normal diet (N=3) or ketogenic
650 diet from 30 weeks of age (N=3) were stained with anti-Ki67 (E). Graph F shows the number of
651 total versus Ki67-positive nuclei from 4 islets. Data are represented as the mean fold expression ±SD.
652 **G, H.** HE-stained pancreatic sections of 45-week-old *Men1*$^{f/f}$-RipCre^{+} mice fed a normal diet (N=4)
653 or *Men1*$^{f/f}$-RipCre^{+} mice fed a ketogenic diet from 30 weeks of age (N=4) were analyzed as shown in
654 Fig. 4B. The numbers of vessels are shown in graph H. Data are represented as the mean fold
655 expression ±SD.
656
657 **Fig. 6 Ketogenic diet suppresses pituitary NET development.**
658 **A.** Pituitary sections of 45-week-old wild-type mice fed a normal diet, *Men1*$^{f/f}$-RipCre^{+} mice fed a
659 normal diet or ketogenic diet from 10 weeks of age were stained with HE.
660 **B.** Pituitary sizes of 45-week-old wild-type mice fed a normal diet, *Men1*$^{f/f}$-RipCre^{+} mice fed a normal
661 diet or ketogenic diet from 10-13 weeks of age were analyzed. Pituitaries of 10-week-old *Men1*$^{f/f}$-
662 RipCre^{+} mice fed a normal diet were also analyzed. Data are represented as the mean fold expression
663 ± SD.
664 **C.** Statistical analysis of the pituitary sizes of each group of mice was performed. P values were
665 obtained using the one-way ANOVA test. The age of the mice sacrificed are shown in parenthesis.
666 **D, E.** Pituitary sections of 45-week-old wild-type mice fed a normal diet and *Men1*$^{f/f}$-RipCre^{+} mice
667 fed a ketogenic diet from 13 weeks of age were stained with anti-prolactin (D) and anti-TSH (E)
668 antibodies.
669 **F.** Pituitary sizes of 55-week-old *Men1*$^{f/f}$-RipCre^{+} mice fed a normal diet or ketogenic diet from 10-13
670 weeks of age were analyzed and compared to those of 45-week-old mice. The data for the 45-week-
671 old mice is the same as in Fig. 6B. Data are represented as the mean fold expression ± SD.
672 **G.** Statistical analysis of the pituitary sizes of each group of mice was performed as in C.
673
674 **Fig. 7 The prognosis of PanNET patients having lower blood glucose levels are better than those**
675 **having higher blood glucose levels.**

676 **A.** Overall survival of patients with high and low fasting blood glucose levels (N=54).

677 **B.** Baseline characteristics of patients analyzed are shown.

678 **C.** Chemotherapeutic regimens of patients analyzed are shown.

679

680

681

682

683 **Supplementary Figure legends**

684

685 **Fig. S1 Ketogenic diet suppresses non-functional PanNET development.**

686 Islet areas of 45-week-old wild-type mice fed a normal diet (N=3), *Men1*$^{f/f}$-RipCre^{+} mice fed a normal
687 diet (N=3) or *Men1*$^{f/f}$-RipCre^{+} mice fed a ketogenic diet from 7-11 weeks of age (N=3) were analyzed.
688 Three pancreatic sections were analyzed for each mouse. The distance between the first and the third
689 section is more than 20 μm. The percentages of islet areas within the total pancreas areas are shown.
690 Data are represented as the mean fold expression ± SD.

691

692 **Fig. S2 Ketogenic diet results in lower blood glucose levels.**

693 Blood glucose levels of 20-week-old male *Men1*$^{f/f}$-RipCre^{+} mice fed a normal diet (N=6) or 40-week-
694 old female *Men1*$^{f/f}$-RipCre^{+} mice fed a ketogenic diet from 10 weeks of age (N=5). Blood glucose
695 levels at basal, after fasting (overnight) and after re-feeding the usual meal for 1.5 hrs were analyzed.
696 Data are represented as the mean fold expression ± SEM.

697

698 **Fig. S3 Ketogenic diet does not affect *Cdkn1b* (p27) mRNA expression.**

699 Islets were isolated from 45-week-old *Men1*$^{f/f}$-RipCre^{+} mice fed a normal diet (N=6) or
700 *Men1*$^{f/f}$-RipCre^{+} mice fed a ketogenic diet from 10 weeks of age (N=5). mRNAs were purified and
701 expression of *Cdkn1b* (p27) was analyzed. Data are represented as the mean fold expression ± SD.

702

703 **Fig. S4 Ketogenic diet suppresses non-functional PanNET progression.**

704 Islet areas of 45-week-old *Men1*$^{f/f}$-RipCre^{+} mice fed a normal diet (N=4) or *Men1*$^{f/f}$-RipCre^{+}
705 mice fed a ketogenic diet from 30 weeks of age (N=4) were analyzed as in Fig. S1.
706 Three pancreatic sections were analyzed for each mouse. Data are represented as the mean fold
707 expression ± SD.

708

709 **Fig. S5 Kaplan–Meier plots of overall survival of the *Men1*$^{f/f}$-RipCre^{+} mice.**

710 In total, 28 male and 42 female *Men1*$^{f/f}$-RipCre^{+} mice fed a normal diet were analyzed.

711

712 **Fig. S6 Blood glucose levels of the patient with or without prior surgery.**

713 In total, 54 patients with (n=21) or without (n=33) prior surgery were analyzed. Data are represented
714 as the mean fold expression ± SEM.

715

716

Fig. 1

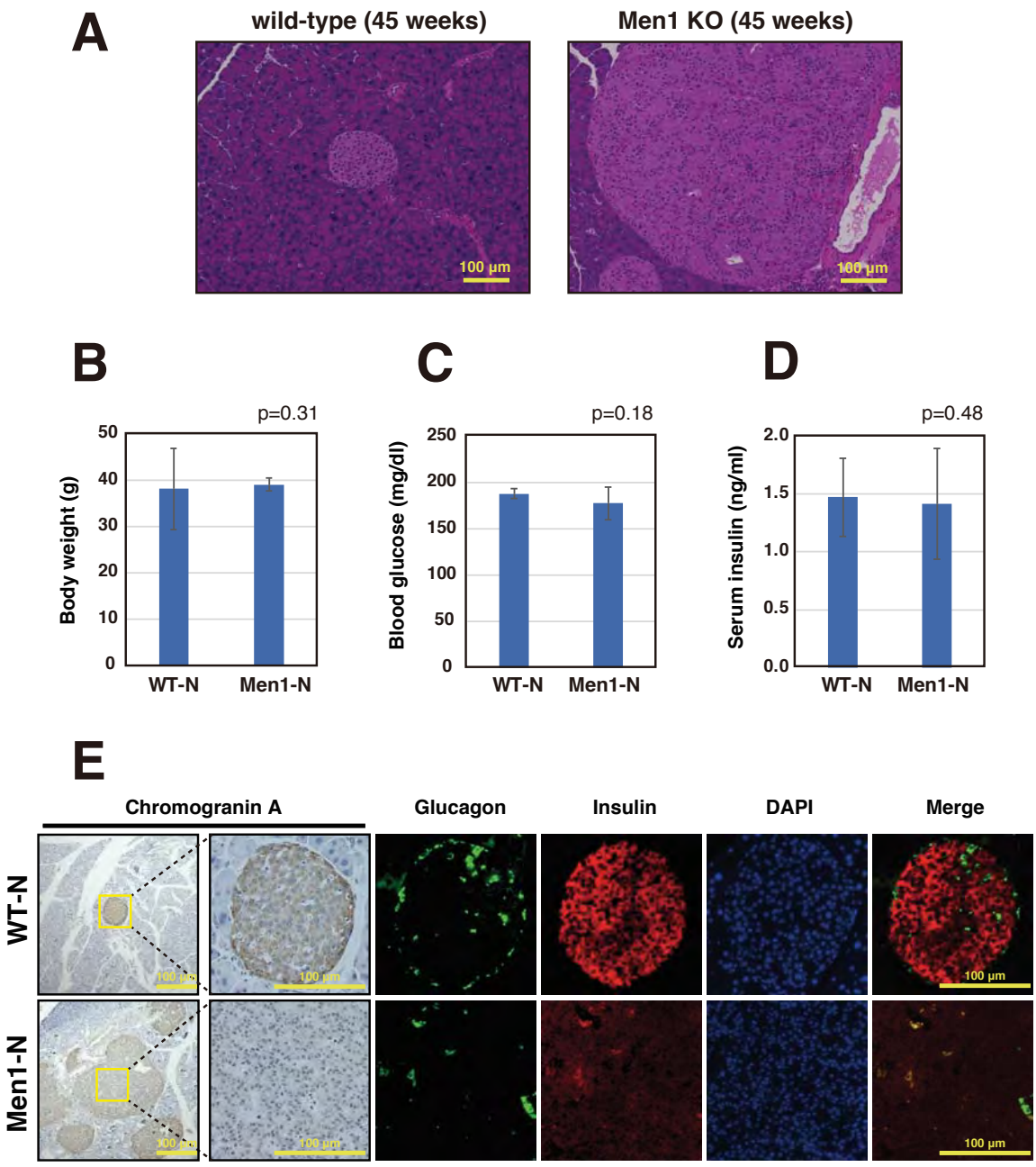
A
wild-type (45 weeks)
Men1 KO (45 weeks)
100 μm
100 μm
B
p=0.31
Body weight (g)
50
40
30
20
10
0
WT-N
Men1-N
C
p=0.18
Blood glucose (mg/dl)
250
200
150
100
50
0
WT-N
Men1-N
D
p=0.48
Serum insulin (ng/ml)
2.0
1.5
1.0
0.5
0.0
WT-N
Men1-N
E
Chromogranin A
Glucagon
Insulin
DAPI
Merge
WT-N
Men1-N
100 μm
100 μm
100 μm
100 μm
100 μm
100 μm
100 μm
100 μm

Fig. 2

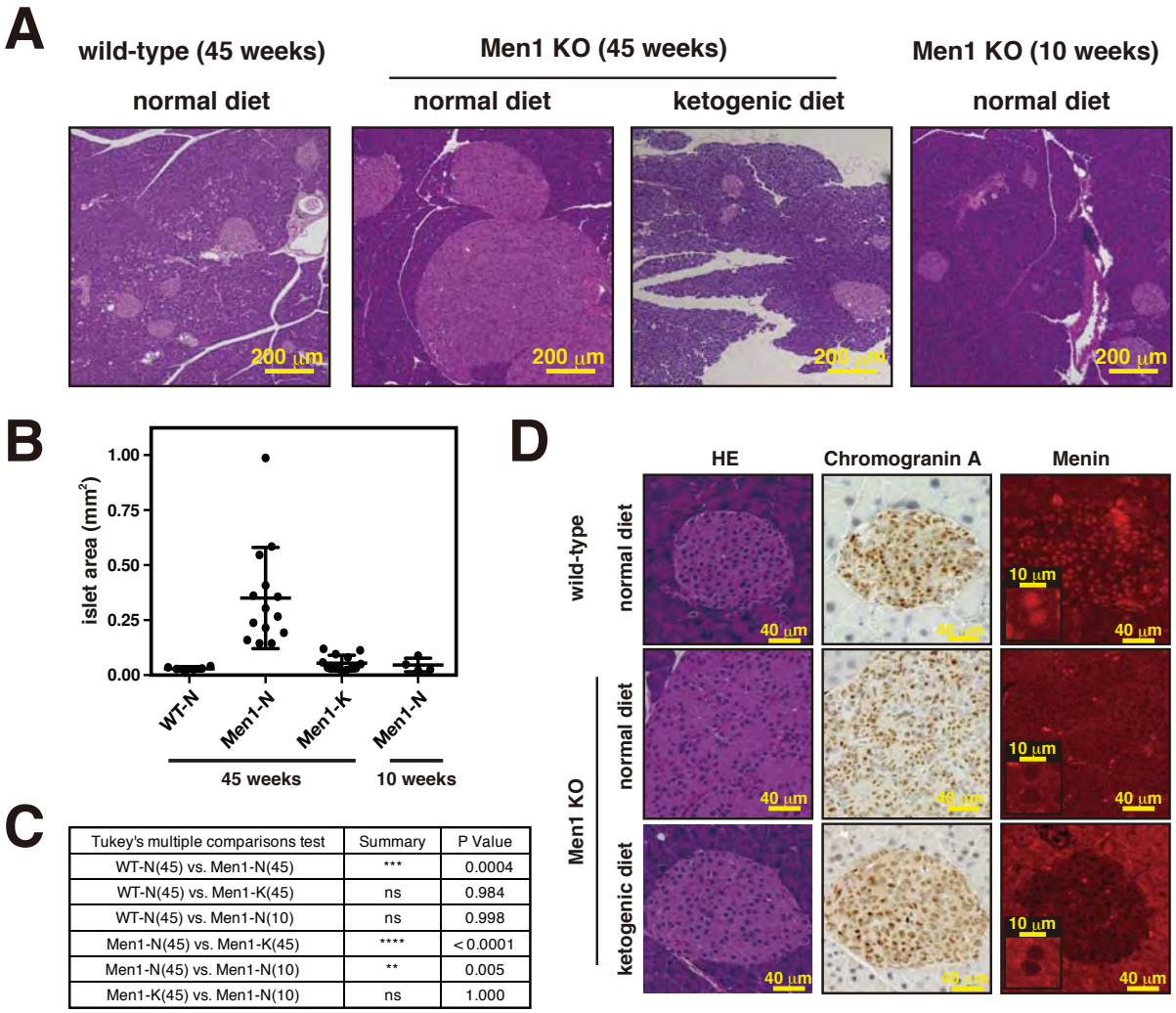

Tukey's multiple comparisons test	Summary	P Value
WT-N(45) vs. Men1-N(45)	***	0.0004
WT-N(45) vs. Men1-K(45)	ns	0.984
WT-N(45) vs. Men1-N(10)	ns	0.998
Men1-N(45) vs. Men1-K(45)	****	< 0.0001
Men1-N(45) vs. Men1-N(10)	**	0.005
Men1-K(45) vs. Men1-N(10)	ns	1.000

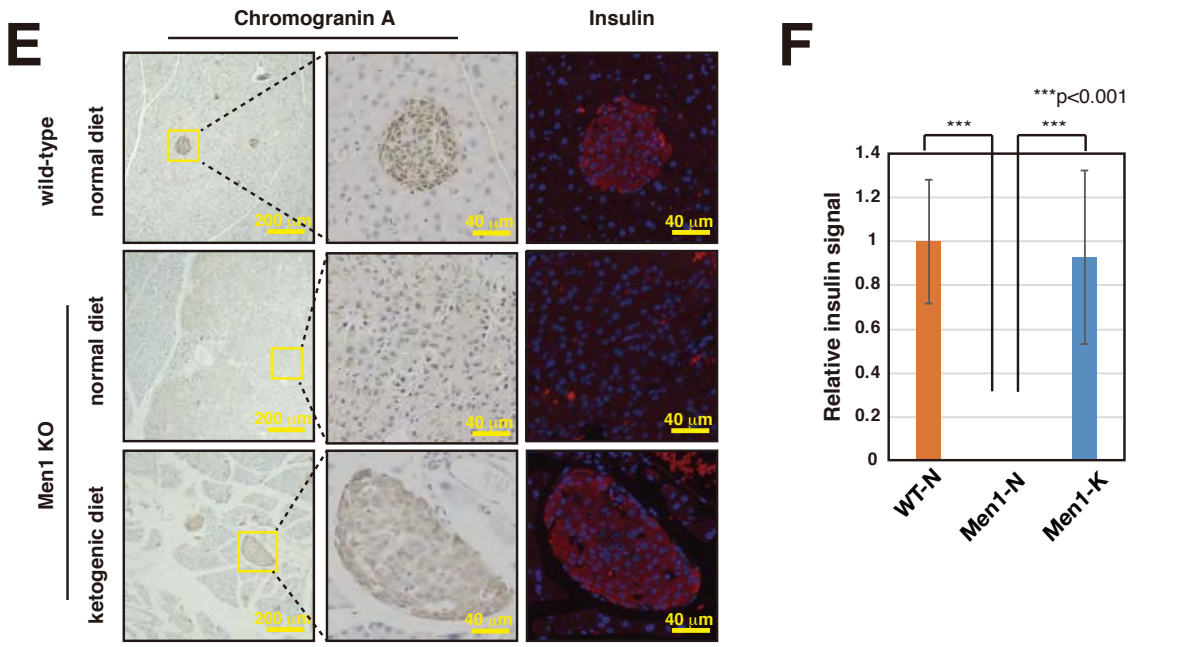

Fig. 3

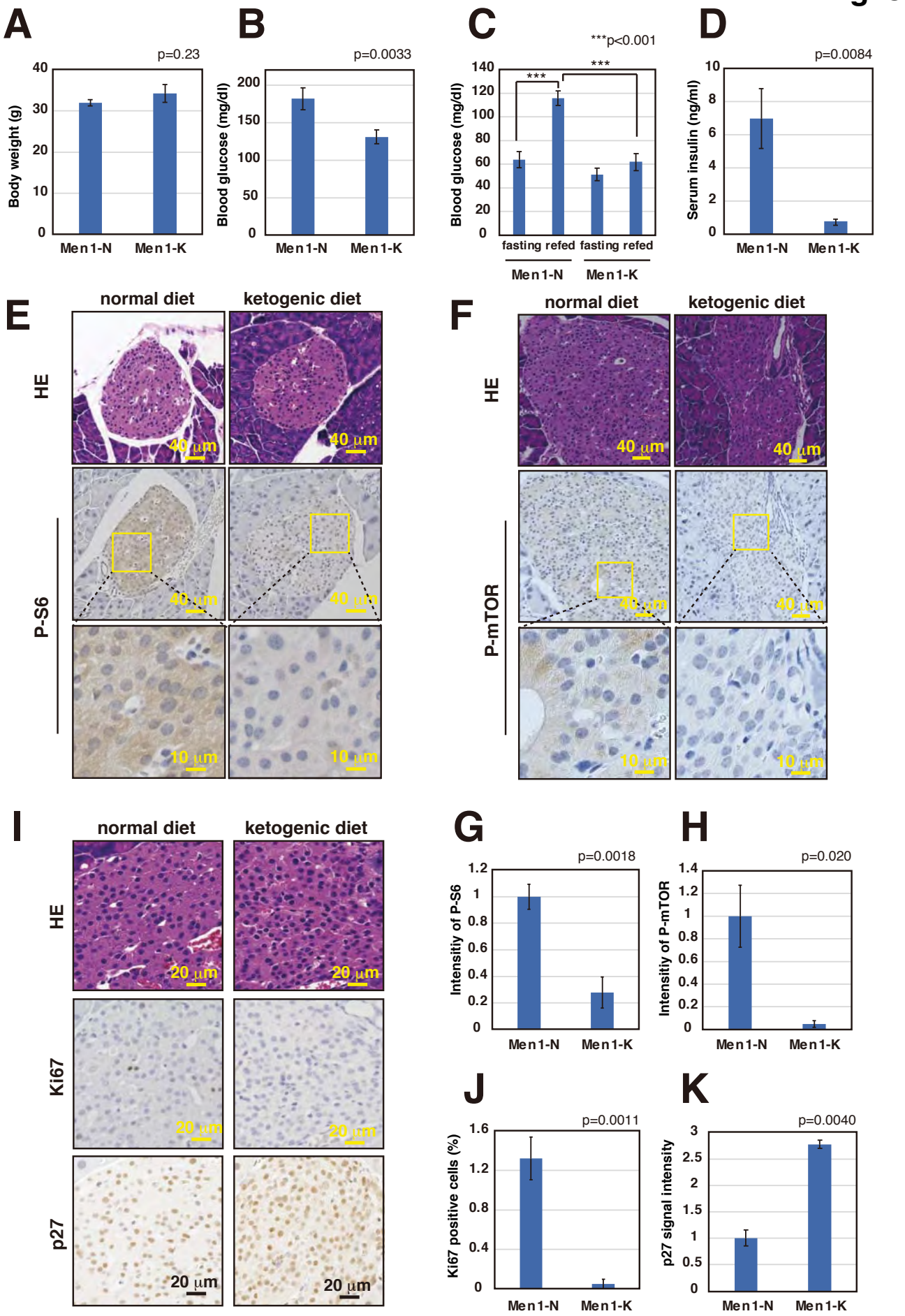
A
p=0.23
Body weight (g)
40
30
20
10
0
Men1-N
Men1-K
B
p=0.0033
Blood glucose (mg/dl)
200
150
100
50
0
Men1-N
Men1-K
C
***p<0.001
***
***
Blood glucose (mg/dl)
140
120
100
80
60
40
20
0
fasting refed fasting refed
Men1-N
Men1-K
D
p=0.0084
Serum insulin (ng/ml)
10
8
6
4
2
0
Men1-N
Men1-K
E
normal diet
ketogenic diet
HE
P-S6
40 μm
10 μm
F
normal diet
ketogenic diet
HE
P-mTOR
40 μm
10 μm
I
normal diet
ketogenic diet
HE
Ki67
p27
20 μm
G
p=0.0018
Intensitiy of P-S6
1.2
1
0.8
0.6
0.4
0.2
0
Men1-N
Men1-K
H
p=0.020
Intensitiy of P-mTOR
1.4
1.2
1
0.8
0.6
0.4
0.2
0
Men1-N
Men1-K
J
p=0.0011
Ki67 positive cells (%)
1.6
1.2
0.8
0.4
0
Men1-N
Men1-K
K
p=0.0040
p27 signal intensity
3
2.5
2
1.5
1
0.5
0
Men1-N
Men1-K

Fig. 4

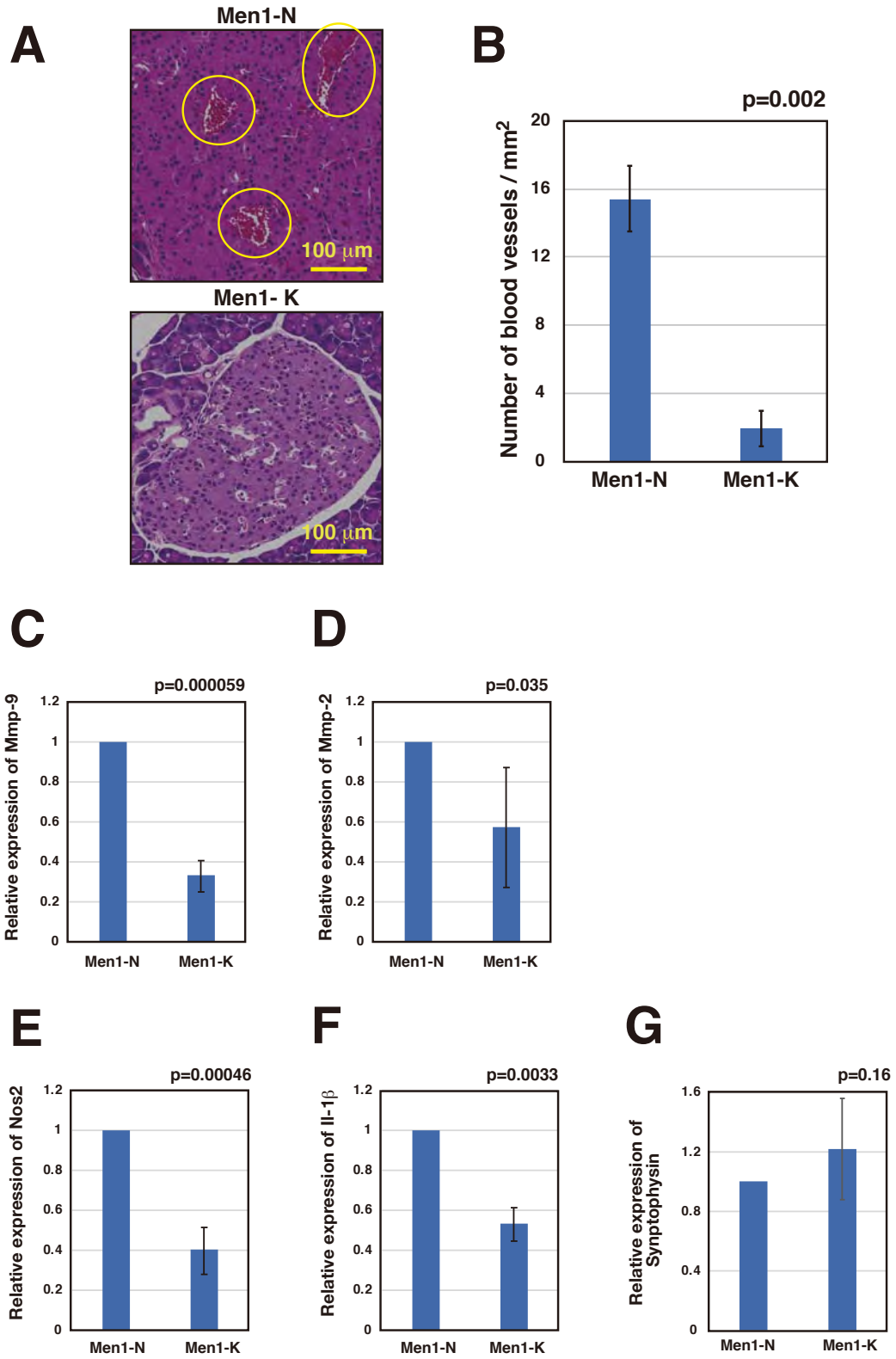
A
Men1-N
100 μm
Men1- K
100 μm
B
p=0.002
Number of blood vessels / mm2
20
16
12
8
4
0
Men1-N
Men1-K
C
p=0.000059
Relative expression of Mmp-9
1.2
1
0.8
0.6
0.4
0.2
0
Men1-N
Men1-K
D
p=0.035
Relative expression of Mmp-2
1.2
1
0.8
0.6
0.4
0.2
0
Men1-N
Men1-K
E
p=0.00046
Relative expression of Nos2
1.2
1
0.8
0.6
0.4
0.2
0
Men1-N
Men1-K
F
p=0.0033
Relative expression of Il-1β
1.2
1
0.8
0.6
0.4
0.2
0
Men1-N
Men1-K
G
p=0.16
Relative expression of Synptophysin
1.6
1.2
0.8
0.4
0
Men1-N
Men1-K

Fig. 5

A

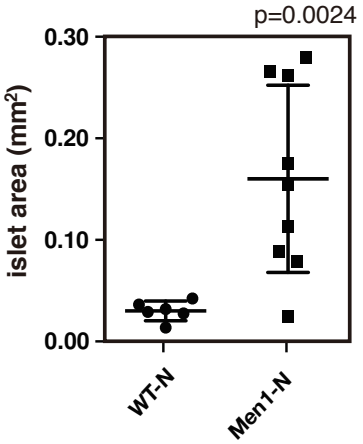

B

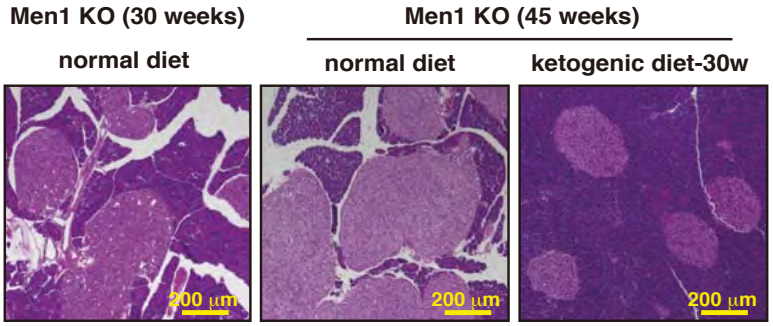

C

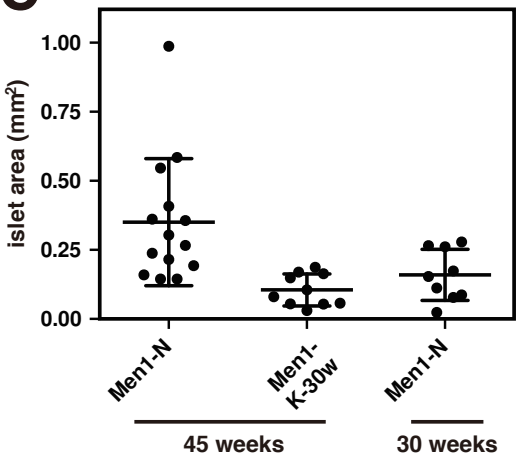

D

Tukey's multiple comparisons test	Summary	P Value
Men1-N(45) vs. Men1-K-30w(45)	**	0.003
Men1-N(45) vs. Men1-N(30)	*	0.026
Men1-K-30w(45) vs. Men1-N(30)	ns	0.748

E

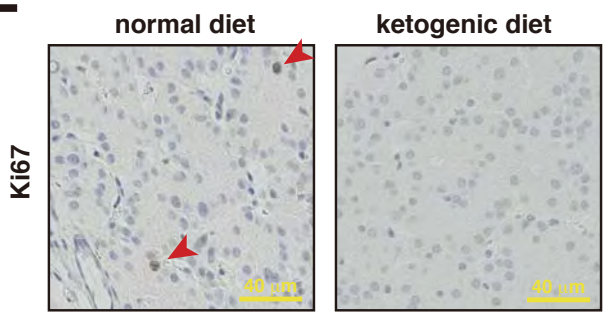

F

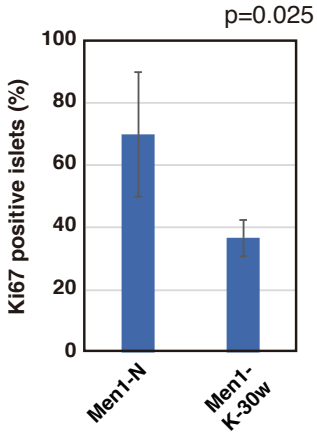

G

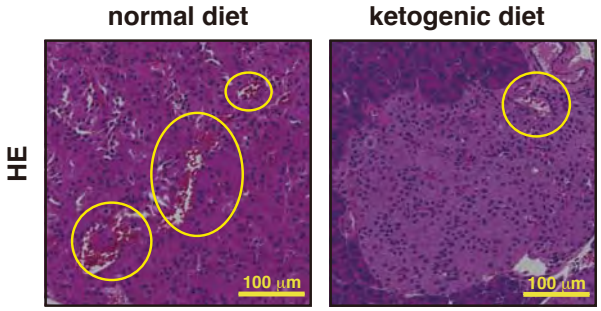

H

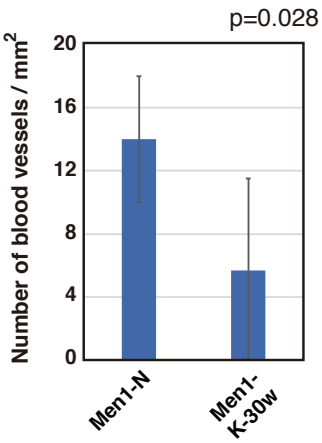

Fig. 6

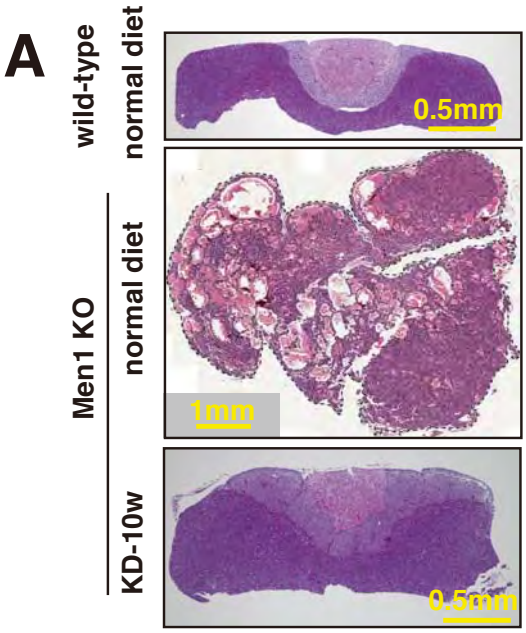

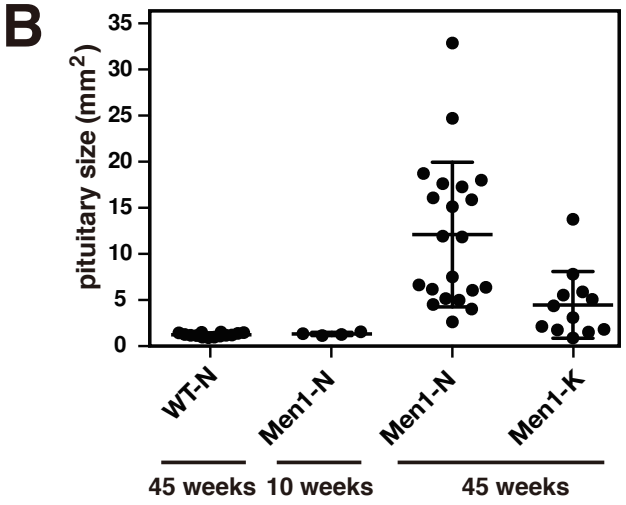

C

Tukey's multiple comparisons test	Summary	P Value
WT-N(45w) vs. Men1-N(10w)	ns	> 0.9999
WT-N(45w) vs. Men1-N(45w)	****	< 0.0001
WT-N(45w) vs. Men1-K10w(45w)	ns	0.4324
Men1-N(10w) vs. Men1-N(45w)	***	0.0036
Men1-N(10w) vs. Men1-K10w(45w)	ns	0.7475
Men1-N(45w) vs. Men1-K10w(45w)	***	0.0017

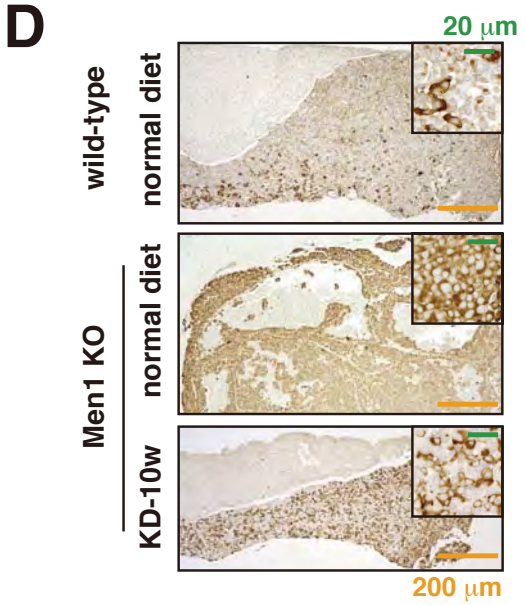

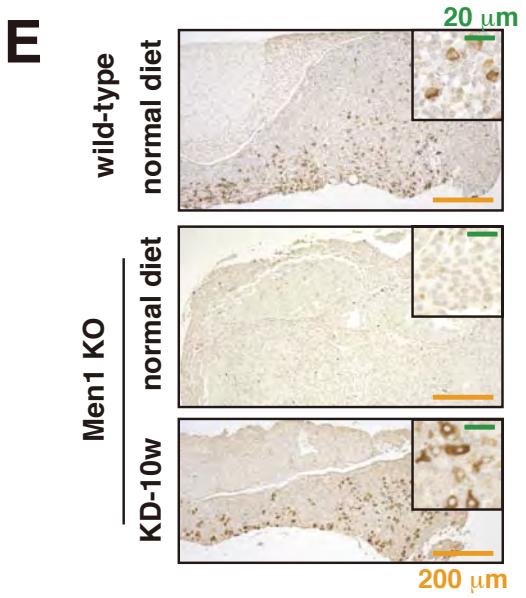

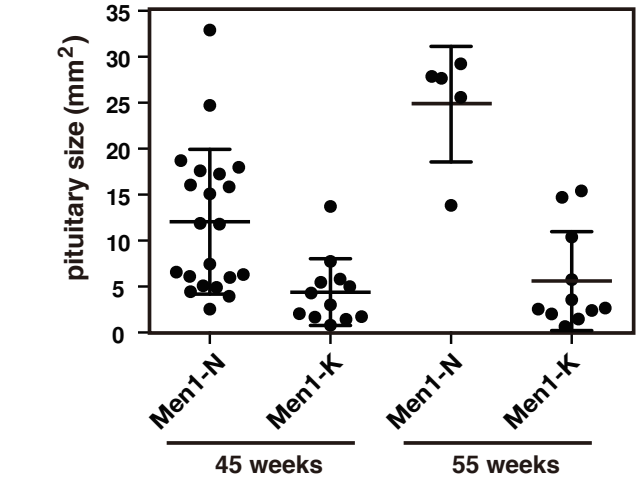

G

Tukey's multiple comparisons test	Summary	P Value
Men1-N(45w) vs. Men1-K-10(45w)	**	0.0094
Men1-N(45w) vs. Men1-N(55w)	**	0.0012
Men1-N(45w) vs. Men1-K-10w(55w)	*	0.0444
Men1-K-10w(45w) vs. Men1-N(55w)	****	< 0.0001
Men1-K-10w(45w) vs. Men1-K-10w(55w)	ns	0.9688
Men1-N(56-59w) vs. Men1-K-10w(55w)	****	< 0.0001

Fig. 7

A

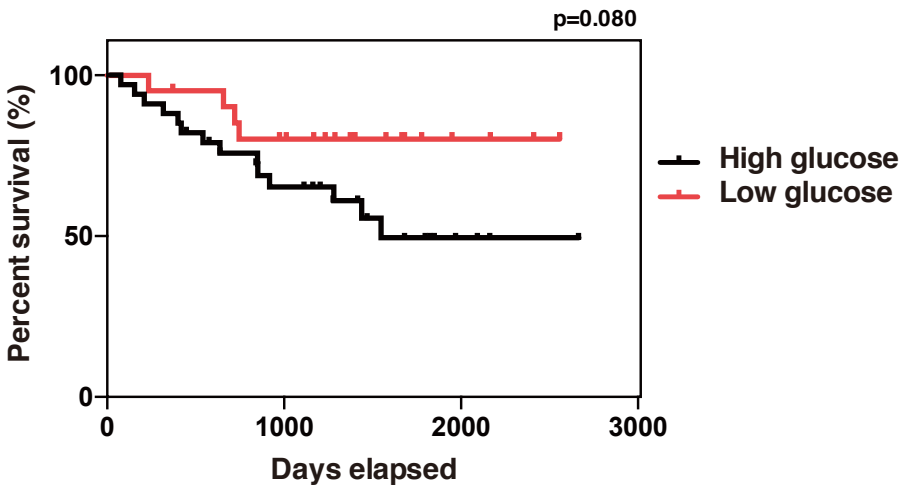

B

Parameters	Blood glucose		p value
	high (n=33)	low (n=21)	
Sex, n (%)			
Male	15 (68%)	7 (32%)	p=0.41
Female	18 (56%)	14 (44%)	
Age, n (%)			
<median (61 years)	17 (65%)	9 (35%)	p=0.58
≧median (61 years)	16 (57%)	12 (43%)	
Tumor grade, n (%)			
G1	3 (67%)	1 (33%)	
G2	24 (57%)	18 (43%)	p=0.78
G3	6 (75%)	2 (25%)	

C

Treatment, n (%)	Blood glucose	
	high (n=33)	low (n=21)
octreotide	3 (100%)	0 (0%)
lanreotide	11 (61%)	7 (39%)
everolimus	8 (80%)	2 (20%)
sunitinib	2 (67%)	1 (33%)
streptozotocin	4 (57%)	3 (43%)
lanreotide+everolimus	3 (60%)	2 (40%)
lanreotide+sunitinib	0 (0%)	4 (100%)
others	2 (67%)	1 (33%)